Optical properties of Cr^{3+} doped $Na_5Lu_9F_{32}$ single crystals grown by the Bridgman method*

ZHAO Zhi-wei (赵志伟)[1], **XIA Hai-ping** (夏海平)[1]**, **HU Jian-xu** (胡建旭)[1], **ZHANG Jian-li** (章践立)[1], **ZHU Yong-sheng** (朱永胜)[2] , **and CHEN Bao-jiu** (陈宝玖)[3]

1. *Key Laboratory of Photo-electronic Materials, Ningbo University, Ningbo 315211, China*
2. *College of Physics and Electronic Engineering, College of Chemistry and Pharmaceutical Engineering, Nanyang Normal University, Nanyang 473061, China*
3. *Department of Physics, Dalian Maritime University, Dalian 116026, China*

(Received 22 March 2018; Revised 17 April 2018)

The growth of $Na_5Lu_9F_{32}$ single crystals doped with Cr^{3+} ions in 0.1 mol%, 0.2 mol% and 0.5 mol% concentrations by Bridgman method was reported. The optical absorption and luminescence spectra decisively demonstrate that the Cr dopant enters $Na_5Lu_9F_{32}$ as Cr^{3+}. Fluorescence emission at wavelengths of 418 nm, 444 nm, 653 nm and 678 nm can be observed under the excitation of 372 nm and the fluorescence lifetime at 418 nm was measured to be ~10.31 μs. The possible crystal sites for Cr^{3+} ions in $Na_5Lu_9F_{32}$ single crystal were discussed, and the lattice parameter *Dq*, Racach parameters *B* and *C* were estimated.

Document code: A **Article ID:** 1673-1905(2018)05-0355-4

DOI https://doi.org/10.1007/s11801-018-8043-8

Solid-state laser diodes with the wide applications such as environment monitoring, military weapons, remote sensing and medical treatment due to the easy manipulation and miniaturization have been a research hotspot in the last decades[1-3]. Transition metal ion doped single crystals as the gain media have been applied to the fabrication of tunable lasers, such as Ti^{3+}:Al_2O_3 and Cr^{3+}:Al_2O_3 sapphire lasers[4]. Among the transition metal ions, the Cr^{3+} ion is an important central luminescent ion and has two characteristic absorption peaks at ~470 nm ($^4A_2 \rightarrow {}^4T_1$) and ~670 nm ($^4A_2 \rightarrow {}^4T_2$)[5]. The reported Cr^{3+} ions doped tunable laser materials include Cr^{3+}:$MgWO_4$, Cr^{3+}:$LiSrAlF_6$ and Cr:LiSAF crystals, etc[6-8]. The search of suitable laser materials is still in progress as the traditional Nd^{3+}:YAG laser used for medical cosmetology operating at 1 060 nm can cause side-effects on human skin. Meanwhile, intense luminescence at ~670 nm emitted by Cr^{3+} ions is skin-safe, which can be employed to develop lasers for medical cosmetology[9]. The previous investigation on the Cr^{3+} ion doped materials mainly focused on oxide single crystals. $Na_5Lu_9F_{32}$ fluoride single crystal becomes the research interest due to the excellent optical transmittance, low phonon energy and long lifetime of the excited state[10-12]. The structure of $Na_5Lu_9F_{32}$ fluoride single crystal provides suitable sites of occupation by trivalent rare earth or transition metal ions. The high transparency and efficient luminescence of the fluoride single crystal make it more favorable as the host material for practical applications than oxide single crystals. In recent years, there have been publications on the growth of rare earth doped $Na_5Lu_9F_{32}$ single crystals[11]. Nevertheless, the growth of Cr^{3+} ion doped $Na_5Lu_9F_{32}$ single crystals of high optical quality remains a challenge. In this paper, we report the growth of Cr^{3+} ion doped $Na_5Lu_9F_{32}$ single crystals by an improved Bridgman method and a preliminary assessment of their optical properties.

The Bridgman technique was used to grow Cr^{3+} ions doped $Na_5Lu_9F_{32}$ single crystals with 99.999% pure NaF, LuF_3 and CrF_3 powders as raw materials. The molar composition of the raw materials was $40NaF\text{-}(60-\chi)LuF_3\text{-}\chi CrF_3$ (χ=0, 0.1, 0.2, 0.5). A seed of $Na_5Lu_9F_{32}$ single crystal along *c*-axis direction was placed at the bottom of the platinum crucible. The temperature gradient near the solid-liquid interface was about 70—90 °C/cm, and the seeding temperature was about 850—870 °C. The growing process was carried out by lowering the crucible at a rate of 0.05 mm/h. The detailed process of crystal growth was described in other reports[11]. The grown crystals were about 50 mm in length and 10 mm in diameter as shown in Fig.1(a). They were light green and transparent. The crystals were cut into pieces and well-polished by CeO_2 powder on both sides to 2.0-mm-thick for optical measurements. Crystal

* This work has been supported by the National Natural Science Foundation of China (Nos.51772159, 51472125, 11504188 and U1504626), the Natural Science Foundation of Zhejiang Province (No.LZ17E020001), and K.C. Wong Magna Fund in Ningbo University.

** E-mail:hpxcm@nbu.edu.cn

structures of the samples were investigated by the X-ray diffraction (XRD) using a Bruker D8 Advance (Germany). The absorption spectra were measured by a Cary 5000 UV/VIS/NIR spectrophotometer. The emission spectrum was recorded under the excitation of 372 nm light by a Triax 320 spectrometer. The fluorescence lifetime was acquired with an FLSP920 fluorescence spectrophotometer. All the measurements were conducted at room temperature with the same condition.

Fig.1(b) presents XRD measurement at room temperature of 0.5 mol% Cr^{3+} doped $Na_5Lu_9F_{32}$ crystal. XRD diffraction peaks and relative intensity of the sample are in good agreement with the standard XRD pattern without any obvious shift, which indicates the crystal structure of the matrix is not significantly changed after Cr^{3+} ion doping. The cell parameters of the crystal are calculated to be $a=b=c=0.546\ 3$ nm from the measured XRD patterns.

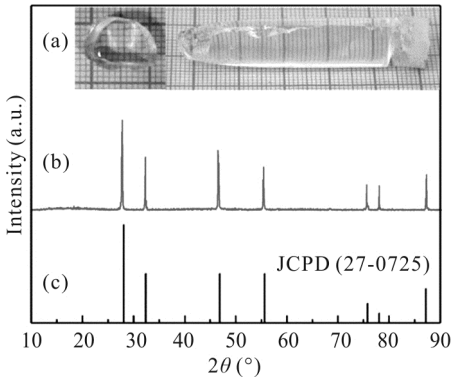

Fig.1 (a) Photo of the grown Cr^{3+}:$Na_5Lu_9F_{32}$ single crystal; (b) XRD pattern of Cr^{3+}:$Na_5Lu_9F_{32}$ single crystal; (c) Standard line pattern of the $Na_5Lu_9F_{32}$ (JCPDS 27-0725)

Fig.2 shows the absorption spectra of the 0.5 mol% Cr doped and the un-doped $Na_5Lu_9F_{32}$ crystals in the wavelength range from 200 nm to 1 200 nm measured at room temperature. The absorption intensity is magnified by a factor of 20 from 600 nm to 1 200 nm in Fig.2. There are two broad absorption peaks in the ultra-violet (UV) range at 259 nm and 372 nm. Also, a weak absorption peak is observed at 670 nm. The enhancement of absorption intensity is consistent with the increase of doping concentration in the grown crystals (other concentrations are not shown in Fig.2). The Cr ion commonly presents two valence states (Cr^{3+} and Cr^{4+}) when doped into various hosts, while Cr^{3+} ion shows most stable properties[13]. The valence is mainly determined by the coordination environment around Cr ions[13]. Previous reports on the absorption of Cr^{4+} and Cr^{3+} ions suggest that a typical absorption peaked at 1 μm is commonly observed according to the crystal-field theory[14,15], which is not observable in Fig.2. Meanwhile, the 259 nm, 372 nm, 663 nm and 670 nm bands shown in Fig.2 are very similar to the absorption characteristics of Cr^{3+} ion, corresponding to $^4A_2\rightarrow b^4T_1$, $^4A_2\rightarrow a^4T_1$, $^4A_2\rightarrow{}^2E$ and $^4A_2\rightarrow{}^4T_2$, respectively[16]. Therefore, it is rational to assume Cr ions in $Na_5Lu_9F_{32}$ crystals as Cr^{3+}. There are two possible crystal sites (Na^+ and Lu^{3+}) for Cr ion to substitute when it is introduced into the$Na_5Lu_9F_{32}$ crystal. The crystal structure of $Na_5Lu_9F_{32}$ can be inferred from Ref.[17], which is in resemblance to CaF_2. The $Na_5Lu_9F_{32}$ crystal in the microscopic condition has a cubic cell with the unit cell parameters of $a=b=c=0.546\ 3$ nm (space group Fm3m). The coordination number of both Na^+ and Lu^{3+} is 8 surrounded by F^- ions. It is well established that the cations with similar radius and valence to Cr ion are more likely to be substituted[16]. The radii of Lu^{3+}, Na^+, Cr^{3+}, and Cr^{4+} are 97.7 pm, 118 pm, 72 pm and 41 pm, respectively. Apparently, the radius difference between Lu^{3+} and Cr^{3+} is the minimum. Meanwhile, charge compensation is not required for Cr^{3+} to replace Lu^{3+} when substitution takes place as both ions have the same valence. Hence, the possible crystal sites for Cr^{3+} to occupy to form stable crystal structure are Lu^{3+} sites.

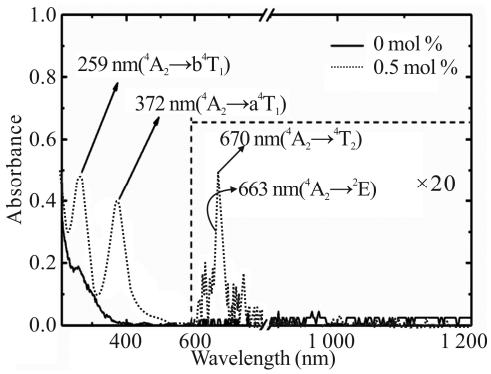

Fig.2 Absorption spectra of $Na_5Lu_9F_{32}$ single crystals doped with 0 mol% and 0.5 mol% Cr^{3+} concentrations

The coordination number of cation in the ionic crystal structure is mainly governed by the ratio of the radius between the positive ion and negative ion. The ratio value ranging from 0.732 to 1 is considered to form stable cubic crystal structure surrounded by eight F^- ligands. The ionic radius ratio between Cr^{3+} (72 pm) and F^- (131 pm) is 0.55. The deviation from the mentioned range indicates that a distorted crystal structure is formed when Cr ions are introduced into the crystal. The previous investigation demonstrates that Cr^{3+} ion in MgF_2, CaF_2, CdF_2, CaF_2, SrF_2 and BaF_2 hosts tends to attract six of the fluorine atoms and push two of them further out, resulting in nearly octahedral coordination as the rather large difference in ionic radius is tolerant to some degree of relaxation. The Cr^{3+} was found to be six-coordinated in the fluorite hosts although the metal sites of the crystal lattices are eight-coordinated. Furthermore, the obtained energy level well agrees with Tanabe-Sugano diagram in octahedral symmetry[16]. In summary, different radii (72 pm for Cr^{3+} vs. 97.7 pm for Lu^{3+}) and similar crystal structure between $Na_5Lu_9F_{32}$ and CaF_2 imply a six-coordinated octahedron structure in the $Na_5Lu_9F_{32}$ for

Cr^{3+} ions.

The parameter of the octahedral crystal-field *Dq* and the Racah parameter *B* for Cr^{3+} doped $Na_5Lu_9F_{32}$ crystal can be calculated by the following equations[18]:

$$E(^4A_2 \rightarrow {}^4T_2)=10Dq \ , \quad (1)$$

$$B=0.33(2\nu_1 - \nu_2)\delta / (9\nu_1 - 5\nu_2) \ , \quad (2)$$

$$E(^2E) / B = 3.05(C / B) + 7.9 - 1.8(B / Dq) \ , \quad (3)$$

where ν_1 and ν_2 are the energy levels of the $^4A_2 \rightarrow {}^4T_2$ and $^4A_2 \rightarrow a^4T_1$ transitions, respectively, δ is the energy difference between the two mentioned transitions, and $E(^2E)$ is the value of energy for the ^2E energy level. Solving Eqs.(1)—(3), the listed parameters for Cr^{3+} in $Na_5Lu_9F_{32}$ crystal can be obtained: *Dq*=1 492.5 cm^{-1}, *B* = 915.9 cm^{-1}, *Dq/B* = 1.63, *C* = 2 904.6 cm^{-1}. The lattice field type is usually determined by the ratio between the lattice field parameter (*Dq*) and the Racah parameter (*B*). If *Dq/B* > 2.3, the medium belongs to the strong lattice field, and sharp emission peaks are expected. A moderate lattice field is indicated if the ratio is about to 2.3. Broad emission peaks resulting from weak lattice field are observed when the ratio is less than 2.3. The calculated *Dq/B* value in our system is less than 2.3, which implies that the $Na_5Lu_9F_{32}$ medium provides a weak lattice field environment for Cr^{3+}. The Tanabe-Sugano diagram of Cr^{3+} in $Na_5Lu_9F_{32}$ single crystal can be obtained based on the value of *Dq/B* and is shown in Fig.3. Tab.1 lists the lattice parameters for other Cr^{3+} ion doped crystals.

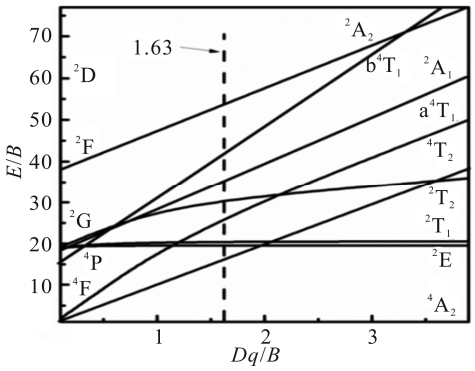

Fig.3 Tanabe-Sugano diagram in octahedron (redrawn from Ref.[16]) for Cr^{3+}

Tab.1 The lattice parameter *Dq*, Racach parameters *B* and *C* of Cr^{3+} ions in different crystals

Crystal	Coordination number	*Dq*/cm^{-1}	*B*/cm^{-1}	*C*/cm^{-1}	*Dq*/*B*
MgF_2[19]	6	1 494	1 038	4 366	1.44
CdF_2[20]	6	1 520	790	3 160	1.92
YSZ[21]	8	1 484.8	920	3 680	1.61
$Na_5Lu_9F_{32}$	6	1 492.5	915.9	2 904	1.63

Fig.4 displays the excitation spectrum measured from 200 nm to 410 nm for the 0.5 mol% Cr^{3+} doped $Na_5Lu_9F_{32}$ crystal by monitoring the 418 nm emission. Two excitation peaks at 268 nm and 369 nm corresponding to $^4A_2 \rightarrow b^4T_1$ and $^4A_2 \rightarrow a^4T_1$ transitions can be observed. They are very close to the absorption peaks at 259 nm and 372 nm shown in Fig.2.

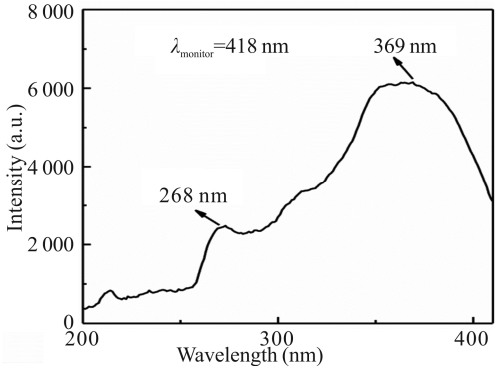

Fig.4 Excitation spectrum of the 0.5 mol% Cr^{3+} doped $Na_5Lu_9F_{32}$ crystal monitored at 418 nm

The emission spectrum scanned from 400 nm to 700 nm of the 0.5 mol% Cr^{3+} doped $Na_5Lu_9F_{32}$ crystal under the excitation of 372 nm is presented in Fig.5. Four characteristic emission peaks at 418 nm, 444 nm, 653 nm and 678 nm corresponding to the $a^4T_1 \rightarrow {}^4A_2$, $^2T_1 \rightarrow {}^4A_2$, $^2E \rightarrow {}^4A_2$ and $^4T_2 \rightarrow {}^4A_2$ transitions, respectively, can be observed. The possible energy transfer mechanisms of Cr^{3+} doped $Na_5Lu_9F_{32}$ single crystal are as follows: the Cr^{3+} ions on the $^4A_2$ ground state were excited to the a^4T_1 energy state by absorbing 372 nm light, and then part of the excited Cr^{3+} ions relaxed radiatively to the $^4A_2$ state with the emission of 418 nm light, while other Cr^{3+} ions decay to the $^2T_1$ level nonradiatively. Subsequently, a portion of Cr^{3+} ions in the $^2T_1$ state transferred energy to the $^4A_2$ state by emitting photons at 444 nm. Another portion of Cr^{3+} ions in the $^2T_1$ state went to the ^2E state without radiation. Following that, ions in the excited ^2E state partly decay to the ground state with 653 nm emission and the remaining ions relaxed to the lowest excited $^4T_2$ state nonradiatively. Finally, Cr^{3+} ions in the $^4T_2$ state transferred to the ground state and emitted 678 nm red light.

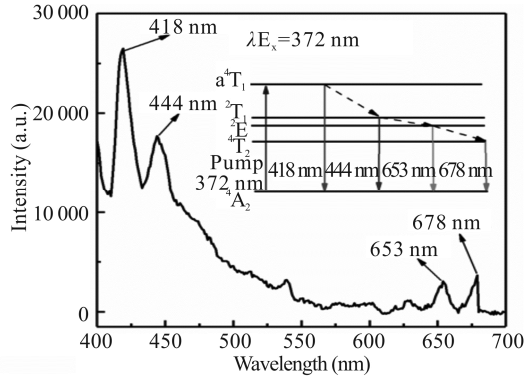

Fig.5 Emission spectrum of the 0.5 mol% Cr^{3+} doped $Na_5Lu_9F_{32}$ crystal under 372 nm excitation (The inset shows the simplified energy level diagram of Cr^{3+}.)

Fig.6 illustrates the decay curve of the $a^4T_1 \rightarrow {}^4A_2$ transition (418 nm) for the 0.5 mol% Cr^{3+} doped $Na_5Lu_9F_{32}$ crystal excited by 372 nm light. Due to the slight nonexponential characteristic of the decay curve, average a^4T_1 lifetime was determined by integrating the entire decay curve according to the expression:

$$\tau = 1/I_0 \int_0^{\infty} I(t)\mathrm{d}t, \quad (4)$$

where I_0 is the luminescence intensity at t=0. The calculated lifetime is 10.31 μs for the 0.5 mol% Cr^{3+} doped $Na_5Lu_9F_{32}$ crystal.

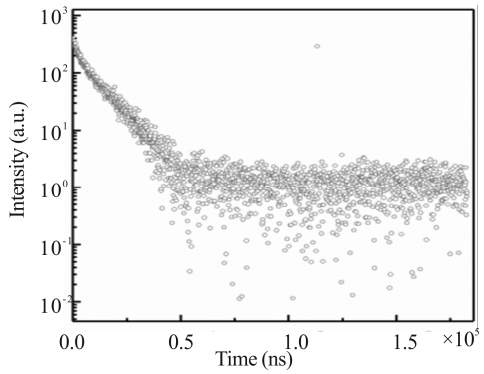

Fig.6 Fluorescence decay curve of the 0.5 mol% Cr^{3+} doped Cr^{3+}:$Na_5Lu_9F_{32}$ crystal monitored at 418 nm under 372 nm excitation

$Na_5Lu_9F_{32}$ crystals doped with various Cr^{3+} concentrations were prepared by Bridgman method. The spectroscopic properties of the grown crystals have been investigated. The crystal field parameter *Dq* and Racah parameters *B* and *C* were calculated as 1 492.5 cm^{-1}, 915.9 cm^{-1}, and 2 904.6 cm^{-1}, respectively. The $Na_5Lu_9F_{32}$ crystal provides a weak crystal field environment for Cr^{3+} ions, and the fluorescence lifetime for the 418 nm emission is about 10.31 μs.

References

[1] Stoeppler G., Parisi D., Tonelli M. and Eichhorn M., Opt. Lett. **37**, 1163 (2012).

[2] Ratnakaram Y. C., Babu S., Bharat L. K. and Nayak C., J. Lumin. **175**, 57 (2016).

[3] Xu J., Kong M., Lin A., Song Y., Han J., Xu Z., Wu B., Gao S. and Deng N., Opt. Lett. **42**, 1664 (2017).

[4] Aggarwal R., Sanchez A., Fahey R. and Strauss A., Appl. Phys. Lett. **48**, 1345 (1986).

[5] Chen D., Chen X., Li X., Guo H., Liu S. and Li X., Opt. Lett. **42**, 4950 (2017).

[6] Zhang L., Huang Y., Sun S., Yuan F., Lin Z. and Wang G., J. Lumin. **169**, 161 (2016).

[7] Demirbas U., Wang J., Petrich G. S., Nabanja S., Birge J. R., Kolodziejski L. A., Kärtner F. X. and Fujimoto J. G., Appl. Opt. **56**, 3812 (2017).

[8] Kunpeng L., Yanlong S., Li Y., Hongwei C., Shaowu C., Mengmeng T. and Aiping Y., Opt. Commun. **405**, 233 (2017).

[9] Huang C., Zhang G., Wei Y. and Huang L., Opt. Commun. **260**, 248 (2006).

[10] Tang Q., Xia H., Sheng Q., He S., Zhang J. and Chen B., J. Mod. Opt. **64**, 2238 (2017).

[11] He S., Xia H., Zhang J., Zhu Y. and Chen B., Sci. Rep. **7**, 8751 (2017).

[12] Sheng Q.-g., Xia H.-p., Tang Q.-y., He S.-n., Zhang J.-l. and Chen B.-j., Optoelectron. Lett. **13**, 201 (2017).

[13] Zhou T., Zhang L., Yang H., Qiao X., Liu P., Tang D. and Zhang J., J. Am. Ceram. Soc. **98**, 2459 (2015).

[14] Ye P., Zhu S., Li Z., Yin H., Zhang P., Fu S. and Chen Z., Opt. Express **25**, 5179 (2017).

[15] Zhou T., Zhang L., Zhang J., Yang H., Liu P., Chen Y., Qiao X. and Tang D., Opt. Mater. **50**, 11 (2015).

[16] Payne S. A., Chase L. L. and Krupke W. F., J. Chem. Phys. **86**, 3455 (1987).

[17] He S., Xia H., Zhang J., Zhu Y. and Chen B., Sci. Rep. **7**, 8751 (2017).

[18] Haiping X., Jinhao W., Hongyin W., Zhang J., Zhang Y. and Tiefeng X., Rare Metals. **25**, 51 (2006).

[19] Nistora R., Andreici L. and Avram N., Acta Phys. Pol. A **19**, 538 (2009).

[20] Gehlhoff W. and Ulrici W., Phys. Status Solidi B **102**, 11 (1980).

[21] Zhang B., Qiu Y., Shen G., He W., Yang B. and Liu J., J. Phys. Soc. Japa. **9**, 1954 (1993).